Two-dimensional DFB laser fabricated on dye-doped hybrid zirconia film by soft lithography

Qiong Zhou (周 琼)[1,4], Sensen Li (李森森)[1], Chaohong Huang (黄朝红)[1], Lujian Chen (陈鹭剑)[1,3*], Huiying Xu (许惠英)[1], and Shou Liu (刘 守)[2]

[1]*Department of Electronic Engineering, Xiamen University, Xiamen 361005, China*
[2]*Department of Physics, Xiamen University, Xiamen 361005, China*
[3]*State Key Lab of Silicon Materials, Zhejiang University, Hangzhou 310027, China*
[4]*Shanghai Institute of Optics and Fine Mechanics, Chinese Academy of Sciences, Shanghai 201800, China*
[*]*Corresponding author: lujianchen@xmu.edu.cn*

Received September 20, 2011; accepted November 11, 2011; posted online January 17, 2012

A two-dimensional (2D) distributed feedback (DFB) structure is fabricated on dye-doped sol-gel derived hybrid zirconia films by soft lithography. The Q-switched Nd:YAG laser (λ = 532 nm) is used to pump these structures. The lasing emissions of the gain medium doped with Rhodamine 6G (Rh6G) in two perpendicular directions are shown, and the threshold pump energy is measured.

OCIS codes: 140.2050, 050.2770, 310.6845.
doi: 10.3788/COL201210.051401.

Organic solid-state gain media have been widely used to fabricate lasers with several kinds of laser resonators, such as distributed feedback (DFB)[1−4], distributed Bragg reflector (DBR)[5], whispering-gallery mode[5], and planar microcavity lasers. Because of its simplicity and low cost, the sol-gel process is suitable for the development of organic gain media in the fabrication of optical elements[6,7]. Zirconia has been used for optical application of sol-gel thin films due to its high refractive index, wide optical transparency in the near-ultraviolet–visible range, and high chemical and thermal stabilities[8].

A DFB laser always consists of a planar or channel waveguide, is mirrorless, and has no external cavity[9]. It is made possible by the presence of periodic perturbations generated from the spatial modulation of the refractive index or the gain, or a combination of both. Typical organic one-dimensional (1D) DFB laser and two-dimensional (2D) DFB laser[10] have been widely reported. Their strong feedback in very compact resonators relies on the refractive index contrast between organic gain material and substrate interface. In contrast to conventional single-grating DFB lasers, dual-grating provides 2D DFB laser structures with superior performance due to stronger photon confinement within the guiding gain region[11].

DFB laser with surface relief structures is conventionally fabricated by a variety of complex methods, including reactive ion etching[12], electron beam lithography, and holographic lithography[13], which require expensive optical and clean room equipment, among others. Alternative techniques such as nano imprinting[14,15], hot embossing, and soft lithography[16,17] have been developed. These techniques are much less expensive and easier to perform. Soft lithography is an alternative, convenient, and less damaging nano-patterning method, and elastomeric molds such as polydimethylsiloxane (PDMS) are employed to pattern materials. PDMS has the several advantages. First, because of its conformal contact with non-planar surfaces without any external force, soft PDMS can replicate a many patterns, whether plane or non-plane. Second, the surface of PDMS has a low interfacial free energy and good chemical stability. Therefore, PDMS elastomers could be easily separated from the replicated structure. Finally, PDMS molds can be used multiple times without noticeable degradation in performance[18].

In this letter, we demonstrate the fabrication of 2D DFB structure on photosensitive dye-doped sol-gel derived zirconia films by soft lithographic method. PDMS elastomer is used to transfer the patterns of holographic grating master to hybrid sol-gel films by soft lithography. We observe lasing emission by pumping the 2D DFB structure in different directions, and measure the threshold pump energy.

Our structures are 2D, second-order periodic gratings. The square lattice is generated on CHP-C positive photoresist by two exposures in a two-beam interferometer (Ar^+ laser, 457.9 nm) separated by a 90° rotation, and finally developed in NaOH solution[17,19,20]. The periods of the gratings can be calculated as[21]

$$\Lambda = \frac{\lambda}{2n_{\mathrm{p}}\sin\Omega}, \quad (1)$$

where n_{p} is the refractive index of CHP-C positive photoresist, λ is the exposure wavelength of 457.9 nm, Ω is the angle between the incident light and the normal line of sample surface, and Λ is the period of the surface-relief gratings (SRGs) obtained. The periods of gratings can be obtained by varying the angle between the two interfering laser beams. In addition, the grating depths are controlled through changing exposure time and development time. The first exposure dose is approximately two times longer than the second exposure dose. Clearly, the grooves of the relief grating become more shallow and the average modulation depth (Δh) is reduced when the exposure dose is decreased.

The flowchart in Fig. 1 shows the fabrication procedure of sol-gel solution. Here, 3-(methacryloxy) propyl trimethoxysilane (MAPTMS) is hydrolyzed with a 0.1-mol/L HCl solution in a molar ratio of 1:0.75, and the mixture is stirred for approximately 15 min. Independently, $Zr(OPr)_4$ and methacrylic acid (MAA) are mixed in a molar ratio of 2.4:1, and stirred for 15 min in 1-propanol solution. MAA reacts to $Zr(OPr)_4$ as a chelating agent, decreasing its reactivity to water. The partially hydrolyzed MAPTMS is then added dropwise to the zirconium solution with continuous stirring for 30 min. Next, DI water is added to the mixed solution, with a final ratio $Zr(OPr)_4$:MAPTMS:H_2O of 0.3:1:3.9. After stirring for another 30 min, the mixture is aged for 48 h in dark place. Rhodamine 6G (Rh6G) is added up to a concentration of 4 mmol/L. A photoinitiator (IRGACURE 819) is added at 2% by weight. The solution is then stirred for an additional 20 min and diluted with optimized amount of 1-propanol before being filtered with a 0.2-μm nylon membrane syringe filter. The thickness of the films could be varied by controlling the solution concentration and the rotation speed in the spin-coating process. In this letter, thin films with thickness of 1 μm could be obtained.

The liquid prepolymer and curing agent (Sylgard 184, Dow Corning) are mixed at a ratio of 10:1 in weight while being fully stirred[22]. The SRGs pattern master is cast with the admixture deflated in a vacuum oven, and cured at approximately 70 °C for 2 h. The 2D DFB structure is then transferred from the master to the PDMS molds. The PDMS stamps are slightly placed onto freshly spin-coated sol-gel films using their own weight. In this process, capillary force allowed the polymer solution to fill the void in the mold, leading to the pattern formation. After prebaking at 60 °C for 15 min and being irradiated with ultraviolet light (10 mW/cm^2), the PDMS molds could be easily separated from the pattern films. The films are postbaked at 120 °C for 1 h.

Figure 2 shows the pumping experimental setup. The

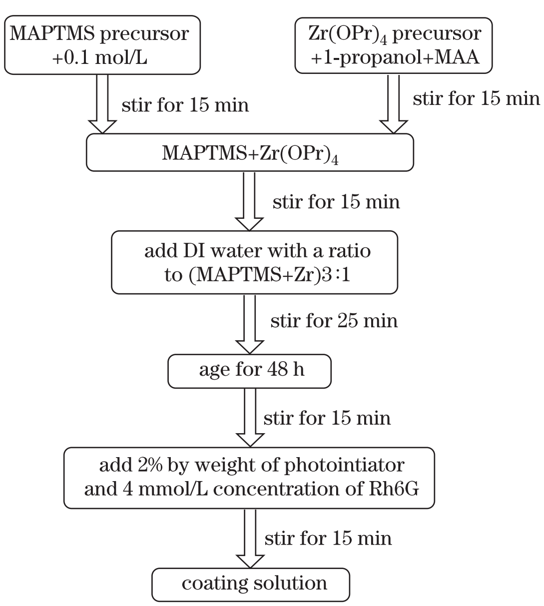

Fig. 1. Flowchart of dye-doped hybrid sol-gel zirconia films preparation.

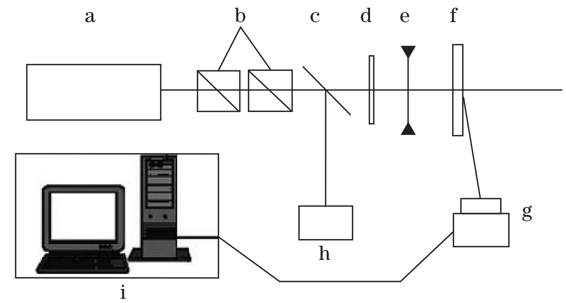

Fig. 2. Diagram of pumping experimental setup. a: Q-switched Nd:YAG laser; b: glan prism; c: reflecting mirror; d: 1/2λ wave plate; e: spherical lens; f: sample; g: high resolution spectrometer; h: powermeter; i: PC.

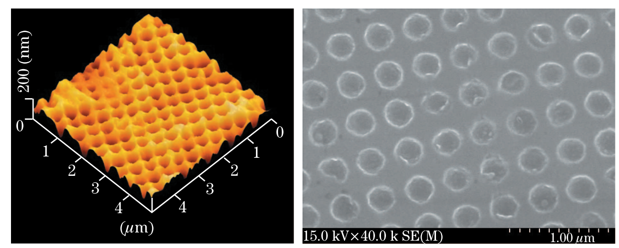

Fig. 3. (a) AFM and (b) SEM images of 2D DFB structure on dye-doped hybrid sol-gel zirconia films.

sample is optically excited with a frequency-doubled, Q-switched Nd:YAG laser (λ= 532 nm, 12-ns pulse width, and 1-Hz repetition rate). At the same time, the pumping energy is monitored using an energy meter (PE10, Ophir Nova). We use a pair of Glan-Taylor prisms to control the polarization and the intensity of pumping beam. The output of the pump laser beam is expanded and collimated by spherical lenses. The emission on the edge of the sample is coupled to a fixed grating spectrometer (HR2000+, Ocean Optics) having a resolution of 0.5 nm through a detection fiber.

The optical properties of the sol-gel derived hybrid film are detected by a commercial prism coupler (Metricon Model 2010) at a wavelength of 633 nm. The refractive index is approximately 1.53 and the thickness is approximately 1.21 μm. The micrographics of the 2D DFB structure are obtained using atomic force microscopy (AFM) in tapping mode and scanning electron microscopy (SEM). As shown in Fig. 3, the 2D structure consists of two perpendicular gratings with grating periods of Λ_1= 422 nm and Λ_2= 429 nm. The measuring results of grating periods are slightly different (~1.7%) due to the low elastic modulus of the Sylgard 184 PDMS used in the soft lithographic technique, which is critical to the replication of SRGs and generation of DFB structures with high fidelity.

We observe lasing emission from the edge of the sample when pumping the 2D DFB structure. As presented in Fig. 4, two sharp lasing peaks with line-width narrow of approximately 0.5 nm can be found in two perpendicular directions. The output laser energy is linearly dependent on the pump energy above the 2-mJ/cm^2 threshold. The beam is highly divergent, which is typical for edge emission from thin films. We attribute the non-uniform intensity variation to the poor edge quality of the device.

A higher index contrast leads to effective coupling of

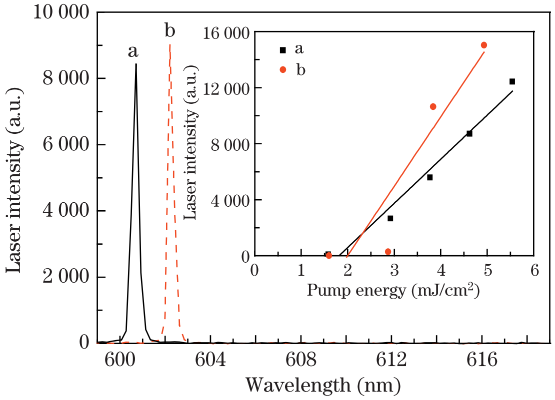

Fig. 4. Laser output spectra for 2D DFB samples in two perpendicular directions under the pump pulse energy of 4.5 mJ/cm^2 with the grating periods of Λ_1=422 nm for a (λ_1=600.7 nm) and Λ_2=429 nm for b (λ_2=602.2 nm). Inset: Laser energy output as a function of pump energy.

the modes in the waveguide laser; thus, feedback is provided. However, the index contrast between glass substrate and the gain material is relatively low because of the low index of the waveguide material composition and the diluted concentration of the dye used here. Hence, a higher out-of-plane loss largely determines a higher lasing threshold, which relates to the radiation modes of substrate and air[23]. This problem can be solved if we fabricate the structure on films with high Zr-Si molar ratio that features a higher refractive index contrast, resulting in a lower threshold.

Lasing occurs near the Bragg resonance, determined by the equation $\lambda_{\mathrm{Bragg}}=2\ n_{\mathrm{eff}}\Lambda/m$, where m is the diffraction order, n_{eff} is the effective refractive index of the propagation mode, and Λ is the grating period. As noted earlier, our 2D DFB lasers utilize a dual-grating structure with an appropriate period selected for second-order operation (m=2). According to the experimental results, the grating with the period of Λ_1=422 nm supports a lasing emission centering at 600.7 nm, whereas the grating with the period of Λ_2=429 nm propagates a laser line at 602.2 nm. Different propagating modes have different values of n_{eff}, which are related to the thickness and refractive indices of the layers that comprise the waveguide. Although the film thickness imposes on the n_{eff} for the guided mode and consequently determines the Bragg resonance, the emission wavelength is consequently affected by thickness variation[24]. The location inaccuracy and repeatability of measuring spot studied here are caused by the error of rotation stages. Therefore, the perturbation of the planar waveguide thickness in different directions leads to the result of close lasing position (~0.3%) with different grating periods (~1.7%). Due to the flexibility of PDMS material, we obtain unequal periods of the 2D DFB lasers despite the SRGs pattern master having equal periods. Furthermore, obtaining a uniform value of n_{eff} is difficult, and the two perpendicular gratings support different laser emission wavelengths. Therefore, a coherent combination of the resonant fields cannot be generated easily[10], resulting in a poor confinement of gain-supported mode. We could choose hard PDMS materials to improve the duplication accuracy, and acquire a 2D DFB laser with the same grating period in perpendicular directions. However, 2D DFB lasers could be designed by tuning the lattice constant in perpendicular directions to achieve two main functionalities of the lasers[25]: one for laser oscillations and the other for efficient light coupling into the device plane. Optical integration is applicable for increasing the emitted intensity and the lasing threshold.

In conclusion, the fabrication procedure of a 2D DFB laser on the dye-doped hybrid sol-gel zirconia film by soft lithography is demonstrated, and the structure is characterized by AFM and SEM. Optically pumped by a frequency-doubled Q-switched Nd:YAG laser, the simultaneous lasing outputs in two perpendicular directions are shown, and the threshold pump energy is measured.

This work was financially supported by the National Natural Science Foundation of China (No. 50802080), the Open Foundation Project of the State Key Lab of Silicon Materials (No. SKL2010-12), and the Natural Science Foundation of Fujian Province, China (No. 2010J01349). The authors thank Prof. Guodong Qian for the prism-coupling measurement, Dr. Jiayu Guo for the SEM study, and Mr. Dingqu Lin for the AFM study.

References

1. A. Jebali, R. F. Mahrt, N. Moll, D. Erni, C. Bauer, G.-L. Bona, and W. Bachtold, J. Appl. Phys. **96,** 3043 (2004).
2. G. A. Turnbull, A. Carleton, G. F. Barlow, A. Tahraouhi, T. F. Krauss, K. A. Shore, and I. D. W. Samuel, J. Appl. Phys. **98,** 023105 (2005).
3. D. Pisignano, M. Anni, G. Gigli, R. Cingolani, G. Barbarella, L. Favaretto, and G. Sotgiu, Synthetic Met. **137,** 1057 (2003).
4. R. Harbers, J. A. Hoffnagle, W. D. Hinsberg, R. F. Mahrt, N. Moll, D. Erni, and W. Bachtold, Appl. Phys. Lett. **87,** 241124 (2005).
5. A. Dodabalapur, M. Berggren, R. E. Slusher, Z. Bao, A. Timko, P. Schiortino, E. Laskowski, H. E. Katz, and O. Nalamasu, IEEE J. Sel. Top. Quantum Electron. **4,** 67 (1998).
6. A.-L. Penard, T. Gacoin, and J.-P. Boilot, Acc. Chem. Res. **40,** 895 (2007).
7. A. Selvarajan and T. Srinivas, IEEE J. Quantum Electron. **37,** 1117 (2001).
8. Y. Sorek, M. Zevin, R. Reisfeld, T. Hurvits, and S. Ruschin, Chem. Mater. **9,** 670 (1997).
9. H. Kogelnik and C. V. Shank, Appl. Phys. Lett. **18,** 152 (1972).
10. G. A. Turnbull, P. Andrew, W. L. Barnes, and I. D. W. Samuel, Appl. Phys. Lett. **82,** 313 (2003).
11. B. J. Scott, G. Wirnsberger, M. D. McGehee, B. F. Chmelka, and G. D. Stucky, Adv. Mater. **13,** 1231 (2001).
12. J. P. Reithmaier and A. Forchel, IEEE J. Sel. Top. Quantum Electron. **4,** 595 (1998).
13. Y. Oki, T. Yoshiura, Y. Chisaki, and M. Maeda, Appl. Opt. **41,** 5030 (2002).
14. E. B. Namdas, M. Tong, P. Ledochowitsch, S. R. Mednick, J. D. Yuen, D. Moses, and A. J. Heeger, Adv. Mater. **21,** 799 (2009).
15. S. Penna, A. Reale, G. M. T. Beleffi, S. Shinada, M. Nakao, N. Wada, A. L. J. Teixeira, and P. S. B. Andre, in *Proceedings of ICTON 2009* Tu.B4.5 (2009).
16. M. Gaal, V. Lavchiev, M. Teuchtmann, H. Schmidt, V.

Rinnerbauer, C. Hasenfuss, H. Plank, G. Mauthner, K. Hingerl, and E. J. W. List, Appl. Phys. A **95,** 265 (2009).
17. J. R. Lawrence, G. A. Turnbull, and I. D. W. Samuel, Appl. Phys. Lett. **82,** 4023 (2003).
18. Y. N. Xia and G. M. Whitesides, Annu. Rev. Mater. Sci. **28,** 153 (1998).
19. G. Langer, A. Pogantsch, K. F. Iskra, T. Neger, and W. Kern, Synthetic Met. **137,** 997 (2003).
20. S. Li, S. Liu, X. Zhang, and X. Ren, Chin. Opt. Lett. **9,** 090603 (2011).
21. C. Ye, K. Y. Wong, Y. G. He, and X. G. Wang, Opt. Express **15,** 936 (2007).
22. L. Wang, W. Jiang, X. N. Chen, L. L. Gu, J. Q. Chen, and R. T. Chen, J. Appl. Phys. **101,** 114316 (2007).
23. A. G. K. Forberich, S. Pereira, J. Crewett, U. Lemmer, M. Diem, and K. Busch, J. Appl. Phys. **100,** 023110 (2006).
24. S. Riechel, U. Lemmer, J. Feldmann, S. Berleb, A. G. Muckl, W. Brutting, A. Gombert, and V. Wittwer, Opt. Lett. **26,** 593 (2001).
25. M. B. K. Christiansen, A. Kristensen, S. Xiao, and N. A. Mortensen, Appl. Phy. Lett. **93,** 231101 (2008).